J Mater Sci (2007) 42:2476–2485
DOI 10.1007/s10853-006-0804-2

Characterization of electrical behaviour of Si modified $BaSnO_3$ electroceramics using impedance analysis

Ashok Kumar · R. N. P. Choudhary

Received: 27 July 2005 / Accepted: 5 December 2005 / Published online: 1 March 2007

Abstract The compounds $BaSn_{1-x}Si_xO_3$ (x = 0–15 mol%) have been prepared by high temperature solid-state reaction route. Powder X-ray diffraction pattern of the samples reveal the formation of a single phase solid solution. It was found that single phase compositions have a cubic crystal structure similar to that of pure barium stannate at room temperature. The a.c. impedance analysis has been carried out in the frequency range 100 Hz–1 MHz for temperature ranging from 300 K to 750 K. Analysis of a.c. impedance data using the complex impedance plane gives the a.c. and d.c. resistance of negative temperature resistance of coefficient (NTCR) electroceramics. Complex impedance plane and complex electric modulus formalism are employed to determine the inhomogeneous nature of the electroceramics. This reveals the presence of single elements in the equivalent circuit at elevated temperature. Grain effects are more prominent than that of grain boundary effect at elevated temperature in the material matrix. The electrical conductivity increases sharply with rise in temperature at elevated temperature due to the thermally activated cations. Master modulus analysis provided an evidence of non-exponential type conductivity relaxation occurring in the materials at higher temperatures.

A. Kumar (✉)
Department of Metallurgy and Materials Engineering, Indian Institute of Technology, Kharagpur 721302, India
e-mail: akumar@metal.iitkgp.ernet.in

R. N. P. Choudhary
Department of Physics and Meteorology, Indian Institute of Technology, Kharagpur 721302, India

Introduction

Now a days electroceramics material with a general formula ABO_3 (A = mono or divalent ions, B = tri, tetra, pentavalent ions) have been widely used for a variety of scientific and industrial applications such as thermally stable capacitor, sensors (gas, humidity), electro-optic devices etc. The physical/electrical properties of this material have been tailored by a suitable choice of cations at the A and B sites [1–5]. It has been found that barium stannate ($BaSnO_3$) in particular has a great significance for some specific applications. An appropriate doping at the Sn site in $BaSnO_3$ is expected to lead to a substantial modification in its structure, thermal, electrical, ferroelectrics and semiconducting properties [6–12]. These electroceramics with high conductivity and moderate activation energy might be useful for electronics application i.e., (fabrication of electrode, resistor and component of heater devices).

In order to complete understanding of electrical conduction mechanism, it is essential to distinguish the grain and grain boundary effects in the material matrix at that particular temperature and frequency domain. For this purpose we have employed complex impedance and modulus analysis. Impedance and modulus analysis are frequently used for analysis of the electrical conductivity of the materials. These are interrelated:

$$M^* = M' + jM'' = j\omega C_0 Z^* = j\omega C_0 (Z' - jZ'') \qquad (1)$$

where, ω is the angular frequency $2\pi f$, M' and M'' are the real and imaginary parts of modulus, Z' and Z'' are the real and imaginary parts of complex impedance, C_0

is the vacuum capacitance of the measuring cell and electrodes with an air gap in place of sample. The equivalent electrical circuit shown below is widely used to represent grain and grain boundary phenomenon in polycrystalline materials. In this equivalent circuit it is desired to separate each of the RC components and measure values. This is seen from the equation for the impedance and modulus of this circuit.

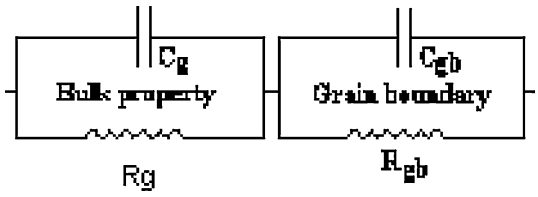

$$Z^* = Z' - jZ'' = (1/R_g + j\omega C_g)^{-1} + (1/R_{gb} + j\omega C_{gb})^{-1} \quad (2)$$

$$Z' = \frac{R_g}{1 + (\omega R_g C_g)^2} + \frac{R_{gb}}{1 + (\omega R_{gb} C_{gb})^2} \quad (3)$$

$$Z'' = R_g \left(\frac{\omega R_g C_g}{1 + (\omega R_g C_g)^2} \right) + R_{gb} \left(\frac{\omega R_{gb} C_{gb}}{1 + (\omega R_{gb} C_{gb})^2} \right) \quad (4)$$

The corresponding equations of M' and M'' are obtained by substituting in to the Eq. 1. These are

$$M' = \frac{C_0}{C_g} \left(\frac{(\omega R_g C_g)^2}{1 + (\omega R_g C_g)^2} \right) + \frac{C_0}{C_{gb}} \left(\frac{(\omega R_{gb} C_{rmgb})^2}{1 + (\omega R_{gb} C_{gb})^2} \right) \quad (5)$$

$$M'' = \frac{C_0}{C_g} \left(\frac{\omega R_g C_g}{1 + (\omega R_g C_g)^2} \right) + \frac{C_0}{C_{gb}} \left(\frac{\omega R_{gb} C_{gb}}{1 + (\omega R_{gb} C_{gb})^2} \right) \quad (6)$$

In the complex impedance plane, a single semicircular arc is seen since the impedance response is dominated totally by that parallel RC element with the larger resistance R_g than that of R_{gb}. In the modulus spectra, a single semicircular arc is seen since the modulus response is dominated by that parallel RC element with the smaller capacitance C_g with respect to C_{gb}. This indicates the material matrix posse's very low capacitance/dielectric constant values. In this way we can say that the exact electrical circuit inside the material matrix is the parallel combination of R_g and C_g at the elevated temperature for pure and modified $BaSnO_3$ at elevated temperature.

The relaxation time was calculated from the peak frequency of Z'' and M'' spectroscopic plots with the help of following relation.

$$2\pi f_{max} RC = \omega_{max} RC = 1 \quad (7)$$

The RC product for each peak is a fundamental parameter, which is the inverse value of f_{max}. This is because the RC product is usually independent of the geometrical factor of the material. It has been observed that the replacement of Sn^{+4} ions in $BaSnO_3$ by other cations (Te^{+4}, Ti^{+4}, Zr^{+4} etc.) of the same group causes a noticeable modification in their electrical properties [13–15]. Further, literature survey reveals that various aspects of physical properties such as microstructure, lattice structure, conduction and dielectric behaviour of $BaSnO_3$/modified $BaSnO_3$ have already been studied [16–19]. However, the electrical properties of Silicon (Si) modified $BaSnO_3$ has not been studied and reported so far. Compared to other thermally stable compound, $BaSn_{1-x}Si_xO_3$ (0–15 wt%) material posses more stable electrical properties because it has not shown any phase transition above room temperature. This aspect has motivated us to undertake the present work comprising a detailed analysis of the effect of Si concentration on the electrical properties of $BaSn_{1-x}Si_xO_3$ (x = 0–15 wt%) using an a.c. technique of impedance analysis.

Experimental

Materials preparation technique

In this present work, the $BaSn_{1-x}Si_xO_3$ (x = 0–15 mol%) electroceramic had been prepared by the high-temperature solid-state reaction method using as precursor salts $BaCO_3$, (99% M/s Glaxo Laboratories, India), SiO_2 (99% M/s Aldrich Chemical Co. Inc., USA) and SnO_2 (99%, M/s Loba Chemical Co.) with the purpose of observing the influence of the Si precursor salt in the $BaSn_{1-x}Si_xO_3$ (x = 0–15 mol%) system. Moreover, the effect of some preparation conditions like drying, thermal aging, calcination and sintering was investigated. The solid solution materials are the ones that present the best oxygen storage capacity, which is very important for the use in the automotives catalysts. The physical mixtures of above ingredients are prepared by mixing the compounds in agate mortar for 2 h. Methanol has been used for the homogeneous mixing of the ingredients. The powder was than calcined in alumina crucible at 1,000 °C for 12 h. The calcined powder was thoroughly mixed

again and recalcined at 1,150 °C for 12 h. The process of grinding and calcinations was repeated until the formation of compounds was confirmed. The calcined powders were cold pressed into cylindrical pellets of diameter 10 mm and thickness1–2 mm with polyvinyl alcohol (PVA) as the binder, using a hydraulic press at a pressure of ~300 MPa. The pellets were then sintered in an air atmosphere at 1,200 °C for 12 h, and then polished with fine emery paper to make their faces flat and parallel. The pellets were finally coated with conductive silver paint and dried at 150 °C for 2 h before carrying out impedance measurements.

X-ray diffraction technique

X-ray diffraction (XRD) studies of the materials were carried out at room temperature in the Bragg angle range $20° \leq 2\theta \leq 80°$ at a scan speed of 2° min^{-1} by an X-ray diffractometer (Miniflex, Rikagu, Japan) using CuKα radiation (λ = 1.5418 Å). The impedance measurements were carried out at an input signal level of 1.5 V in the temperature range of 35–600 °C using a computer-controlled impedance analyzer (HIOKI LCR Hi TESTER, Model: 3532-50) in the frequency range of 100 Hz–1 MHz. along with a laboratory made sample holder and a heating arrangement. The accuracy of the temperature measurement was found about ±0.5 °C.

Results and discussion

X-ray diffraction analysis

Figure 1 shows the X-ray diffraction (XRD) patterns of $BaSn_{1-x}Si_xO_3$ (x = 0–15 mol%) at room temperature, which reveals the formation of single phase compounds. XRD structural study confirmed the cubic symmetry of the compounds at room temperature. The XRD patterns of $BaSnO_3$ are well matched with the internationally recognized JCPDS file [20]. All the diffraction peaks of $BaSn_{1-x}Si_xO_3$ (0–15 mol%) were successfully indexed and the related parameter were evaluated with the computer controlled program POUD [21]. The d-observed (d_{obs}) and d-calculated (d_{cal}) value was well matched having minimum standard deviation in the cubic crystal system. The diffraction peaks shifts toward high Braggs angle side with increasing Si concentration. The intensity of the peaks was found to be increased with increasing Si concentration. The above observations indicate that the Si atoms successfully replaced the Sn atoms from the crystal lattice.

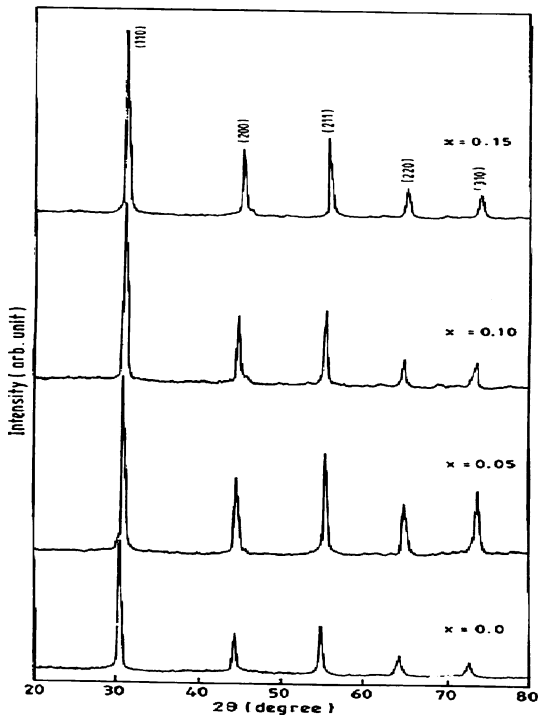

Fig. 1 XRD pattern of $BaSn_{1-x}Si_xO_3$ (x = 0–0.15 mol%) at room temperature

Complex impedance analysis (Nyquist plots)

Typical complex impedance plane plot of $BaSn_{1-x}Si_xO_3$ (0–15 mol%) are given in Fig. 2 at elevated temperature for different Si concentration. At elevated temperature, a more ideally semicircular shape is seen with a small depression, which is the characteristic feature of polycrystalline material. It has been observed that the net impedance value decreases on increasing temperature for all concentration. In case of Si modified $BaSnO_3$ the impedance value decreases sharply at elevated temperature. It can also be observed that the value of impedance decreases with increasing Si concentration and the value of impedance are lower than that of the $BaSnO_3$ at elevated temperature for Si concentration (x = 10 mol%). At elevated temperature, the impedance values of 10 mol% Si modified $BaSnO_3$ gives maximum value. As we increase the molar concentration of Si (above10 mol%) the impedance values slightly increases at elevated temperature. This may be due to the Si uneven (due to higher concentration) distribution inside the crystal lattice. So the critical concentration may be 10 mol% Si for enhancing the conductivity of the materials. In order to analyse and interpret experimental data, it is essential to have a model equivalent circuit that provides a realistic representation of the electrical

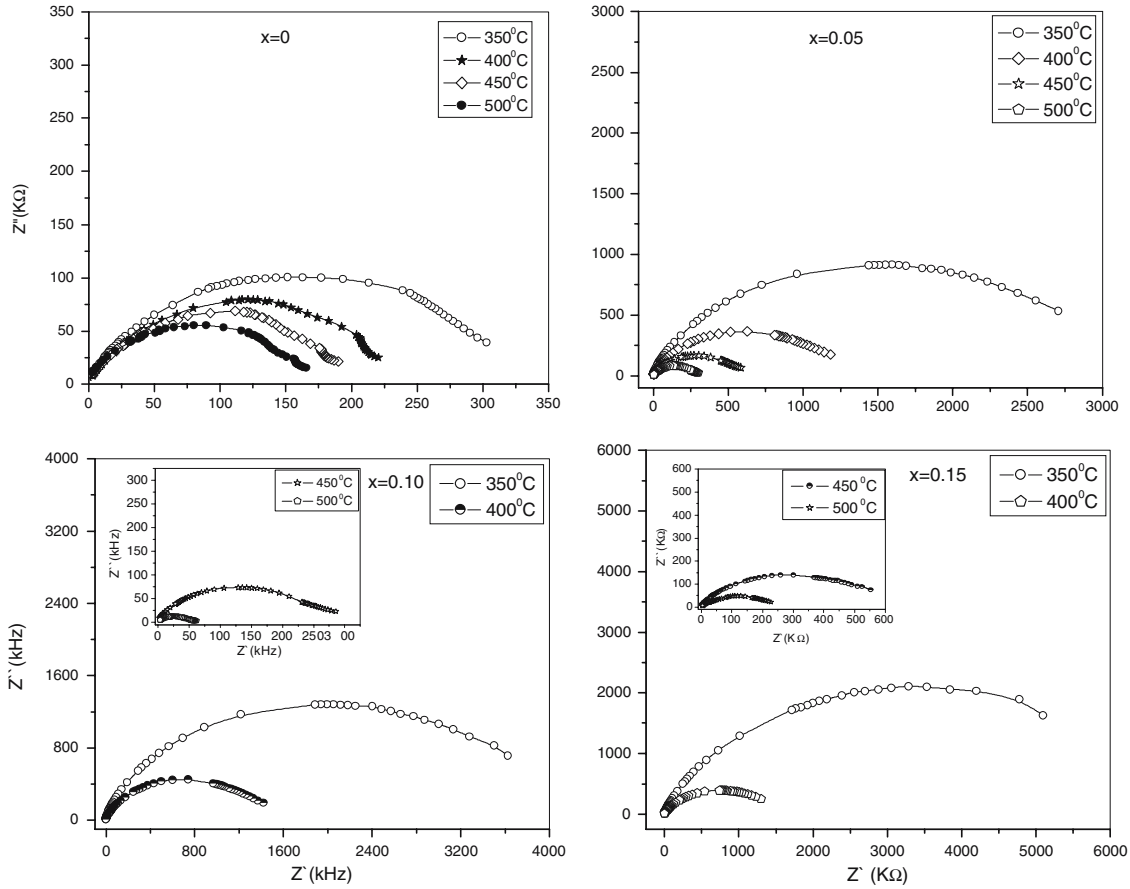

Fig. 2 Complex impedance spectrum (Nyquist plot) of $BaSn_{1-x}Si_xO_3$ (x = 0–0.15 mol%) at different temperature

properties. The equivalent electrical circuit has shown earlier. Figure 2 does not show any grain boundary as well as ceramic electrolyte–electrode interface effect in the material for any Si concentration. On the basis of above observation we can say that the equivalent electrical circuit reduced to the parallel combination of R_g (grain resistance) C_g (grain capacitance) in the material. With the prior observation it can be concluded that the $BaSnO_3$/Si modified $BaSnO_3$ shows negative temperature resistance of coefficient (NTCR) behaviour at elevated temperature [22–26].

The impedance data can be analysed much better way in the modulus formalism methods (Fig. 5). In our case both the method shows the single circular arc for all concentration at elevated temperature. This can be explained that the equivalent circuit at these temperatures appears to contain two parallel RC elements; the resistance as well as capacitance of one is much lower than the other i.e., grain resistance is much higher than that of grain boundary resistance whereas grain capacitance is much lower than that of grain boundary capacitance.

Analysis of complex impedance loss spectra

Figure 3a shows the loss impedance spectra of $BaSn_{1-x}Si_xO_3$ (0–15 mol%) at elevated temperature. It has been seen from the loss spectra that impedance value decreases with increasing temperature for all concentration. The peak relaxation frequency shifted towards higher frequency side with increase in temperature. Only a single relaxation peaks observed for each concentration and temperature. It has been observed that relaxation phenomenon arises in the materials above 300 °C and the value of relaxation time decreases with increasing temperature. The relaxation time obtained from the following relation:

$$\omega_{max}\tau = \omega_{max}RC = 1$$

The activation energy obtained from the relaxation plots are in the range of ~E_a = (~1.0–1.2 eV) for all concentration at elevated temperature which indicates that O^{2-} ions/defects plays predominant role in the conduction mechanism inside the material matrix. The

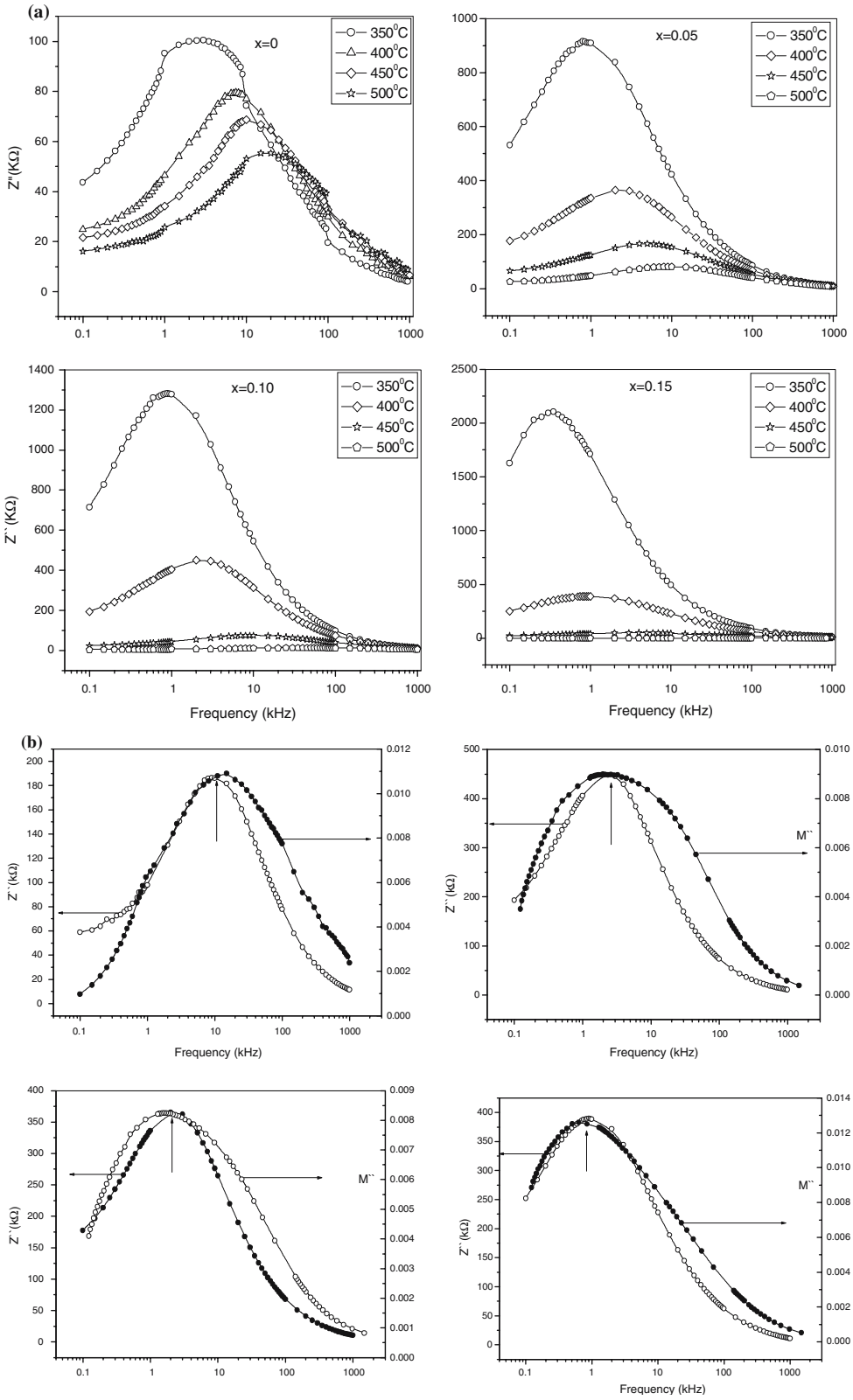

Fig. 3 (**a**) Loss spectrum (Z'' versus frequency plot) of $BaSn_{1-x}Si_xO_3$ (x = 0–0.15 mol%) at different temperature. (**b**) Impedance Z'' and modulus M'' of $BaSn_{1-x}Si_xO_3$ (x = 0–0.15 mol%) as a function of frequency

nature of point defect may be in our specimens is due to oxygen ion vacancy or detachment of the Si^{+4} ions from the crystal lattice at elevated temperature. Since, the materials have been sintered at very high temperature (1,200 °C). These oxygen ion vacancies may be created during sintering process. The activation energy

calculated from conductivity graph also suggests oxygen ion conduction in the material matrix at elevated temperature. $BaSnO_3$ is used a gas sensor (O_2, CO_2, N_2) in which O^{2-} ions take part in the conduction mechanism [Ref. 1–5]. This would imply that the relaxation is temperature dependent and the charge species relaxed within a shorter interval of time. The effect of Si at different site is quite significant as indicated by the changes in the pattern of loss spectra for different compositions of Si when compared with the pattern for $BaSnO_3$. The merger of loss spectra at higher frequency side is an indication of the evidence of space charge in the material that governs electrical process in the region of high frequency.

The spectroscopic plots show a similar effect (Fig. 3b) with a single peak in Z'' and M''. An advantage of a combined M'' and Z'' plot on the same frequency scale is that both M'' and Z'' peaks coincide for a particular RC element. A rapid assessment can therefore be made from a visual inspection of such a combined plot. The time constant for the grain has roughly the same in both impedance and modulus spectra. The two peaks in both Z'' and M'' plot overlap each other. These effects have been seen in the Fig. 3b. Thus modulus plots give most emphasis on those elements with the smallest capacitances where as impedance plots highlight those with the largest resistance.

Electrical conduction behaviour

Figure 4a shows the d.c. conductivity of $BaSn_{1-x}Si_xO_3$ (0–15 mol%) as a function of temperature. The plots indicate that all compounds govern the Motts type electrical conduction behaviour below 350 °C. At the temperature greater than 350 °C, all compounds obey the Arrhenius type thermally activated conduction

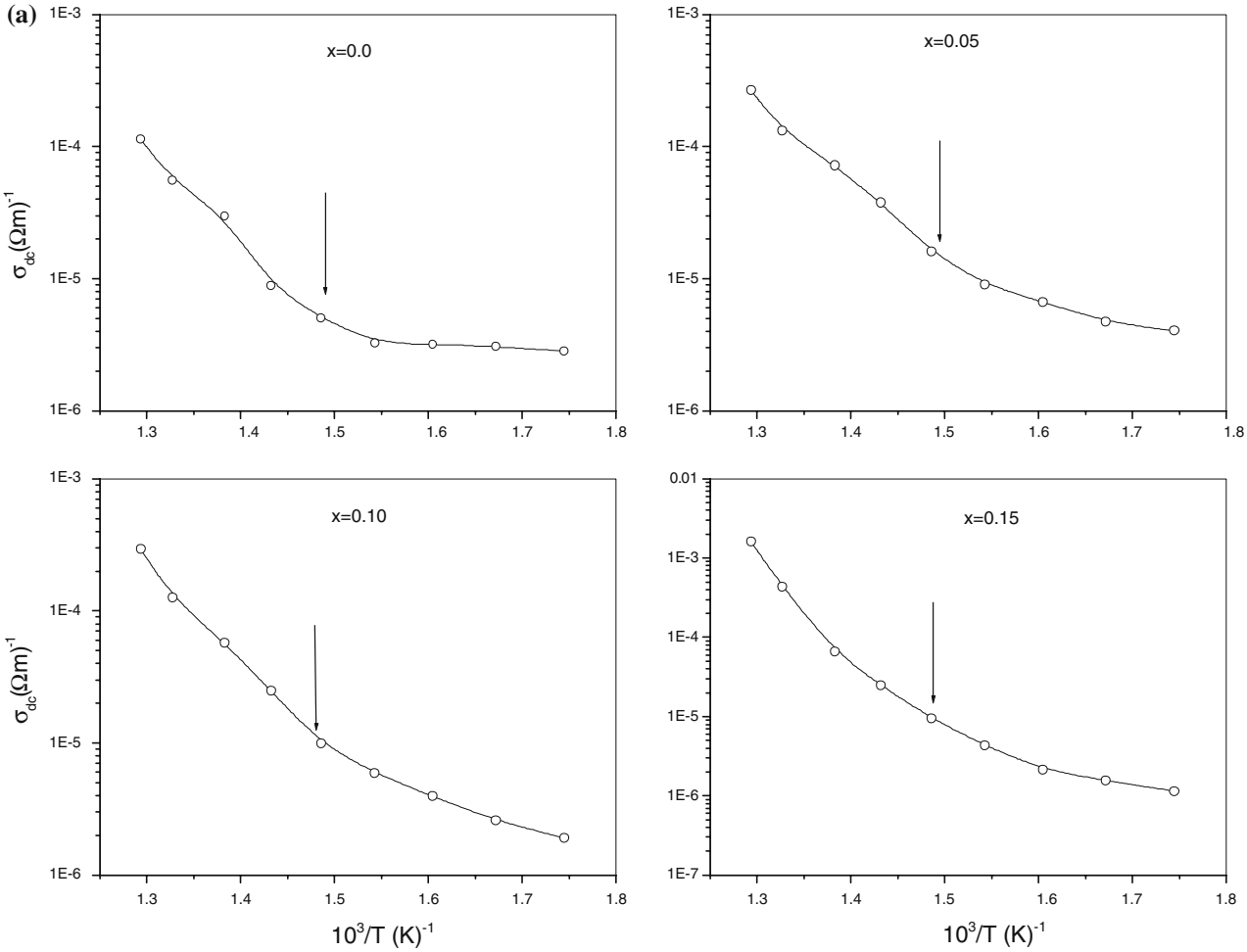

Fig. 4 (**a**) Variation of d.c. electrical conductivity of $BaSn_{1-x}Si_xO_3$ (x = 0–0.15 mol%) as a function of temperature. (**b**) Variation of a.c. electrical conductivity of $BaSn_{1-x}Si_xO_3$ (x = 0–0.15 mol%) as a function of frequency. (**c**) Variation of a.c. electrical conductivity of $BaSn_{1-x}Si_xO_3$ (x = 0–0.15 mol%) as a function of temperature

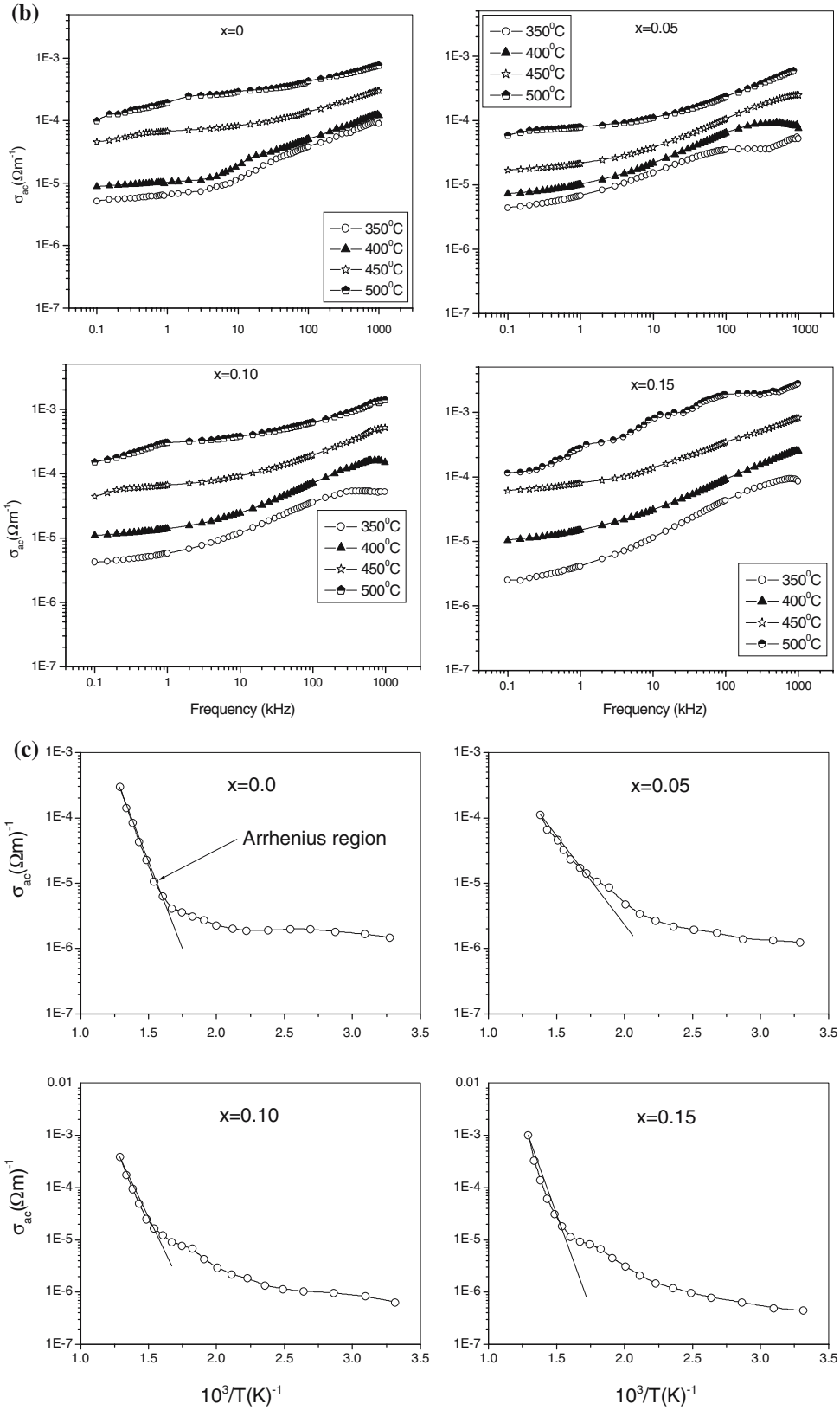

Fig. 4 continued

process. The linear variation at $T > 350$ °C has been well matched to Arrhenius type thermally activated transport of charge carriers governed by the relation:

$$\sigma_{dc} = \sigma_0 \exp\left(-\frac{E_a}{k_B T}\right) \quad (8)$$

where σ_0, E_a and k_B represent the pre-exponential factor, activation energy of the mobile charge carriers and Boltzmann constant, respectively. The activation energy of the material has been estimated to be (~1.0–1.1 eV) at elevated temperatures (i.e., $T > 350$ °C). It indicates the possibility of more than one type of charge carriers taking part in electrical conduction in the material in two different ranges of temperatures. It may be attributed to electrons obeying Mott's behaviour in the low temperature region (i.e., $T < 350$ °C) and Si^{+4}/O^{2-} vacancies/defects in the high temperature region (i.e., $T > 350$ °C). The above mechanism is well supported by the activation energy required for O^{2-} vacancies in the conduction process.

The a.c. conductivity has been measured as a function of frequency at elevated temperatures is shown in the Fig. 4b. At $T > 350$ °C a frequency independent conductivity is observed in low frequency region (≤1 kHz). This frequency independent region shifted towards higher frequency side with increase in temperature. From the above observations it can be concluded that the existence of multiple relaxation and thermally activated charge species in the material is observed. These results are in close agreement with the observations from impedance spectrum analysis. The frequency at which change in slope of the pattern occurs is known as hopping frequency (ω_p) which suggests that the electrical conduction takes place via hopping mechanism governed by the Jonscher's universal power law: $\sigma_{ac} = \sigma_{dc} + A\omega^n$ where A is a thermally activated constant depending upon temperature. The dispersion at lower temperature possibly indicates the space charge of the material that vanishes at higher frequency and temperatures.

Figure 4c shows the variation a.c. conductivity as a function of temperature. It indicates the linear behaviour of conduction in low temperature region ($T \leq 350$ °C) and a non-linear conduction behaviour in the high temperature regions which well obey the Arrhenius type thermally activated conduction process. It is likely that (low temperature region) each response responsible for the different relaxation times have discrete activation energies, thus at different temperatures each will contribute differently to the overall "total" impedance; this is most likely the reason for the non-Arrhenius behaviour observed in low temperature region. Whereas the activation energy calculated in high temperature regions are well matched with the activation energy calculated from d.c. conductivity plots in this particular temperature region.

Complex modulus formalism

Electrical response of the material has also been analysed by complex electric modulus $M^*(\omega)$ formalism [22]. Electric modulus formalism (Fig. 5a) shows the presence of single semicircular arc for all concentration

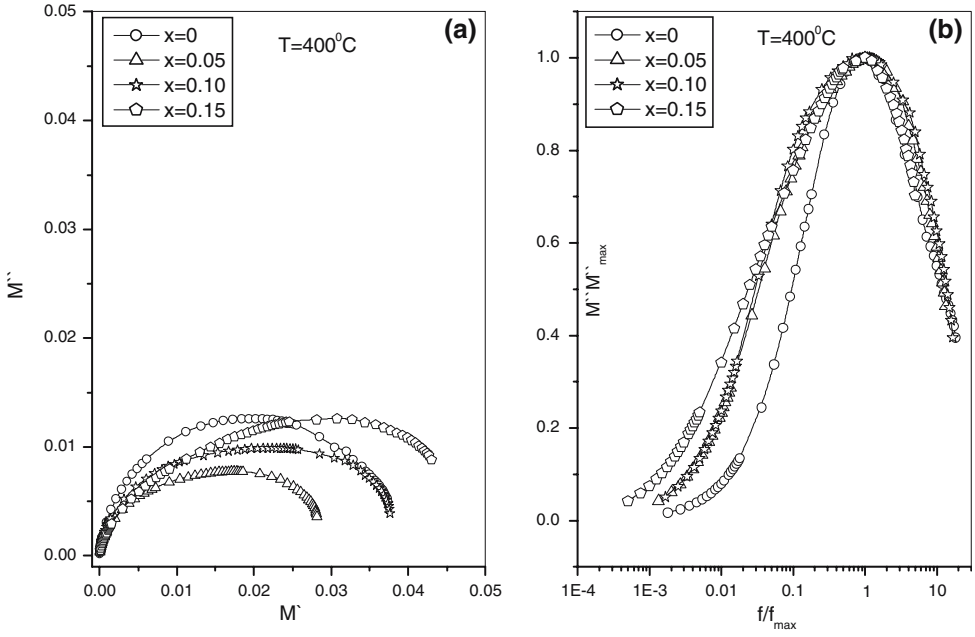

Fig. 5 (**a**) Complex Modulus spectrum of $BaSn_{1-x}Si_xO_3$ (x = 0–0.15 mol%) at elevated temperature. (**b**) Modulus Master Curves (M''/M''_{max} vs. f/f_{max}) of $BaSn_{1-x}Si_xO_3$ (x = 0–0.15 mol%) at elevated temperature

at temperature equal to 400 °C. Similar response has been obtained for all concentration at elevated temperature. The modulus spectra reflects the same nature of plots as that of impedance spectra which reveals that the grain resistance are of the order of 2–3 times greater than that of grain boundary resistance which diminishes the grain boundary effects. Also the grain capacitances are of much lower ($\sim 10^2$–10^3) than that of grain boundary capacitance. Figure 5b shows the variation of normalized complex modulus with f/f_{max} at different temperatures for the $BaSn_{1-x}Si_xO_3$ (0–15 mol%). The modulus master curve enables us to understand the electrical process occurring in the material as a function of temperature. The nature and patterns of master plots are almost similar for all concentration and temperature (>350 °C), which obey non-Debye type conductivity relaxation phenomenon. The concept of non-exponential behaviour and non-Debye process is related with the conductivity relaxation mechanism in which the relaxation process is itself non-exponential due to specific interactions between the relaxing unit and the environment. The master modulus curve that enables us to have an insight into the dielectric processes occurring in the material as a function of temperature. The results indicate the possibility of a non-exponential type conductivity relaxation in the system that can be described by Kohlrauch–Williams–Watts (KWW) function expressed as:

$$\Phi(t) = \exp\left[-\left(\frac{t}{\tau_\sigma}\right)^{\beta}\right]$$

where $\tau_\sigma = \frac{1}{2\pi f}\beta$ $(0 < \beta < 1)$ is the conductivity relaxation time and β Kohlrauch exponent. The smaller the value of β larger is the deviation in the relaxation mechanism compared to Debye type relaxation.

The pattern of variation indicates that appearance of the peak almost at the same frequency for all concentration in the material at a particular temperature. The estimated full width at half maxim (FWHM) from the M''/M''_{max} spectra is wider than the width of a Debye peak (1.14 decade). These results suggest the presence of non-Deby type single relaxation phenomena in the material with marked enhancement in polydispersive behaviour of the materials with Si doping. This confirms suggest the presence of non-Debye type conductive relaxation phenomena in the materials.

Conclusions

XRD studies confirmed the formation of single phase solid solution of system $BaSn_{1-x}Si_xO_3$ (0–15 mol%). A.C. impedance analysis reveals that mostly bulk properties plays predominant role in the conduction mechanism. All the purposed compounds show NTCR behaviour in the whole temperature range. It has been obtained from the master modulus formalism, the bulk capacitance of the materials are 2–3 order lower than the grain boundary capacitance at elevated temperature. Si doped ($x = 10\%$) $BaSnO_3$ shows better electrical conduction at elevated temperature ($T = 500$ °C) than that of undoped $BaSnO_3$. The electric conductivity taken by the impedance analysis suggests Mott's type charge transport at low temperatures and Arrhenius type thermally activated process at high temperatures. A master modulus analysis provides evidence of conductivity relaxation mechanism, which is of non-exponential and non-Debye type at high-temperature region. The activation energy estimated from the conductivity patterns suggests a possibility of the conduction due to oxygen-vacancy at $T > 350$ °C.

References

1. Claessen R, Smith MG, Goodenough JB (1993) Phys Rev B 47(4):1788
2. Udawatte CP, Kakihana M, Yoshimura M (2000) Solid State Ionics 128:217
3. Young LM (1979) J Mater Sci 14:1579
4. Lu W, Jiang S, Zhou D, Gong S (2000) Sensors Actuat A: Phys 80(1):35
5. Licheron M, Jouan G, Husson E (1997) J Eur Ceramic Soc 17:1453
6. Azad AM, Shyam LLW, Yen PT (1999) J Alloys Comp 282:109
7. Jayaraman V, Mangamma G, Gnasekaram T, Periaswami G (1996) Solid State Ionics 86:1111
8. Rai RS, Sharama S, Choudhary RNP (2002) Ferroelectric 275:11
9. Singh NK, Choudhary RNP, (2000) Ferroelectrics 242(1–4):89
10. Ginlely DS, Bright C (2000) Mater Res Soc Bull 25:15
11. Cerda J, Arbiol J, Dezanneau G, Diaz R, Morante JR (2002) Sensors Actuat B4:1
12. Ostrick B, Fleischer M, Lampe U, Meixner H (1997) Sensors Actuat B44:601
13. Shimizu Y, Narikiyo T, Arai H, Seiyama T (1985) Chem Lett 377
14. Keppel A, Meixner H, Mock R (November 1998) (Siemens AG, Germany) US Patent 5840255, 24
15. Ku JK (June 1994) (Sam Hwa Capacitor, Korea), KR Patent 9405 993, 30
16. Kutty TRN, Vivekanandan R (1987) Mater Res Bull 11:1457
17. Parida SC, Banerjee A, Das S, Prasad R, Singh Z, Venugopal V (2002) J Chem Thermodyn 34:527
18. Tao S, Gao F, Liu X, Sorensen OT (2000) Sensors Actuat B 71:223
19. Lampe U, Gerbling J, Meixner H (1995) Sensors Actuat B 24:657

20. JCPDS File No: 15-780
21. POWDMULT: An Interactive Powder Diffraction Data Interpretation and Indexing ProgramVersion 2.1, E.Wu, School of Physical Sciences, Flinder University of South Australia, Bradford Park, SA 5042, Australia
22. Patel HK, Martin SW (1992) Phys Rev B 45:18
23. Sinclair DC, West AR (1989) J Appl Phys 66(8):15
24. James AR, Priya S, Uchino K, Srinivas K (2001) J Appl Phys 90:3504
25. Bahuguna Saradhi V, Srinivas K, Prasad G, Suryanarayana SV, Bhimasankaram T (2003) Mater Sci Eng B 98:10
26. Selvasekarapandian S, Vijaykumar M (2003) Mater Chem Phys 80:30